SSC22-II-05

"Global Navigation Satellite System Performance in Cislunar Space for Cubesat form factors"

"Warren Soh, Sunil Bisnath, Regina Lee, Peter Keum"
"York University"
"102 Campus Walk, North York, ON, Canada" ; +16139867725
wsoh@yorku.ca

ABSTRACT

An increased Cislunar traffic is expected by the end of this decade stemming from NASA's Artermis program. Given the prioritization limitations of the Deep-Space Network (DSN) for ranging and tracking of increased deep-space assets, a more viable, and cost effective, independent navigation capability is needed. NASA's 2015 Navigator Global Positioning System (GPS) deployed on the Magnetospheric Multi-Scale (MMS) spacecraft has validated the feasibility of acquiring weak GPS signals at distances up to 25 Earth Radii (~150,000km) or about 40% of the Cislunar trajectory. NASA plans to upgrade the flight proven MSS Navigator GPS for the future Lunar Gateway. Concurrently, the European Space Agency has confirmed the feasibility of an interoperable GPS and Galileo receiver at Lunar altitudes for a low acquisition and tracking threshold "Weak HEO" receiver for a Cubesat platform. This engineering analysis sets out to explore: (1) the smallest Global Navigation Satellite Systems (GNSS) receiver antenna that can ensure a positive carrier and code link for a Lunar bound Cubesat; (2) the position dilution of precision (PDOP) profile of this Lunar bound space vehicle; and (3) the expected improvement of the PDOP during the Moon Transfer Orbit (MTO) for an interoperable GNSS receiver, specifically Beidou. For the designed carrier-to-noise acquisition and tracking threshold of 15 dBHz, the Eb/N_0 link was assured for a helix antenna with a minimum diameter of 130 mm and length of 200 mm for the GPS L1 frequency at a data rate of 50 bps. The Galileo E5a, E5b would require a larger diameter antenna at 760 mm at 448 bps data rate while Beidou requires a 350 mm diameter antenna for a 100 bps data rate to close their respectively. Utilizing the 130 mm diameter, 200 mm length helix antenna on a Lunar MTO, the preliminary assessment indicated that the GNSS PDOP calculated from valid carrier links increases from 20 when the vehicle is within the GNSS service volume to several 100th or 1000th at 60.3 Earth Radii. Due to their similar constellation altitude geometry, the Galileo E5b PDOP growth profile is similar to that of the GPS L1. The Beidou system however has a much lower PDOP growth. This difference is attributed to the set of Beidou Geosynchronous space vehicles (SV)s that have greater angular separation to the SV-receiver line-of-sight (LoS). For an interoperable GNSS receiver that can track the GPS, Galileo, and Beidou lower bound and upper bound frequencies simultaneously, the increased number of valid signals reduces the PDOP growth below 200. This engineering analysis re-affirms the potential of utilizing existing GNSS infrastructure for onboard navigation in Cislunar space, in particular, a helical antenna that can be accommodated on a Cubesat form factor.

INTRODUCTION

NASA's ambitious Artemis Program to land the first woman and the next man on the Lunar south pole by 2024[1] comes at an opportune time in comparison to its predecessor, the Apollo program. Unlike Apollo that followed 12 years after the launch of Sputnik 1 in 1957, Artemis can now leverage six decades worth of astronautical advancements. One such space technology is the US NAVSTAR Global Positioning System (GPS), the very first Global Navigation Satellite Systems (GNSS). The GPS's original military intentions has proliferated into commercial applications, becoming an indispensable everyday tool, from personal geo-location wearable receivers to precision timing for massive financial trade services. In the last 20 years, GPS receivers have flown on satellites at various altitudes, including Geosynchronous orbits (GSO) at 36,000 km, 1.8 times higher than the GPS satellite constellation residing at 20,200 km altitude. The GOES-16 GSO GPS receiver and antenna system could acquire the GPS transmitted primary lobes when not obscured by the Earth but uses mainly side lobes of the transmitted GPS constellation signals[2]. More recently, the GPS navigation experiment onboard the four Magnetospheric Multi-Scale (MMS) spacecraft had demonstrated the ability to receive GPS signals at extremely high altitudes, 4.6 times higher than GSO[2]. Each spacecraft carries a low Carrier-to-Noise-density ratio (C/N_0) acquisition and tracking threshold 25 dB-Hz GPS receiver with an Ultra Stable Oscillator (USO) coupled to eight high gain 200 mm diameter by 160 mm length GPS antennas mounted on each apex of the octagonal shaped spacecraft. Using NASA Goddard's Enhanced Onboard Navigation System (GEONS) orbit determination filter, the MMS Phase 2 mission had proven that position estimation using GPS signal

sidelobes (Figure 1) was feasible at 150,000 km altitude, approximately 25 Earth Radii (RE) or 40% of the Earth-Moon cislunar space. The MMS Phase 1 mission at 76,000 km altitude was able to filter clock biases to within 15 m root sum squared (RSS) 1-sigmawhile the Phase 2 mission at 150,000 km altitude filtered clock biases within 50 m RSS 1-sigma. It was also noted in the Phase 2 mission that the long-term trend showed an average tracking of 3 GPS signals with up to a maximum of 8 observed sidelobe signals.

Encouraged by the MMS Phase 2 mission, Winternitz[3] assessed the feasibility of deploying the same MMS Navigator GPS System with another USO from Frequency Electronics Inc, and with a 500 mm high gain GPS antenna for NASA's future Lunar Orbital Platform-Gateway (LG) with a target Earth-Moon Lagrange point 2 (L2) Southern Near-rectilinear halo orbit (NRHO). The paper's objective was to investigate a low-cost ranging alternative, and to free up the default two-way ranging system performed by NASA's Deep Space Network (DSN) for all deep-space missions. An error scaling assessment for the in-range and lateral range was formulated as a geometric error metric, confirming the relation that the clock errors were directly proportional to the range squared errors versus the lateral errors. Monte Carlo simulations of the NRHO trajectory for both crewed and uncrewed LG, showed range 3-root mean squared (3-RMS) errors of 202.9 m and 909.7 m respectively and lateral 3-RMS errors of 31.3 m and 79.0 m respectively. This difference was attributed to the modelled jitter disturbances of the crewed system. The study of this new GPS receiver and antenna did not include simulated operations for a trajectory from an Earth parking orbit to the moon, i.e., a Moon Transfer Orbit (MTO), nor were there specific discussions on the acquisition and tracking threshold.

The United Nations Office for Outer Space Affairs (UNOOSA) issued an interoperable GNSS Space Service Volume study in 2018 which included an assessment for signal availability for each individual GNSS and the combined GNSS cases for a simple ballistic cislunar trajectory from LEO to orbit insertion (a "figure 8" trajectory) [4]. For simulated acquisition and tracking thresholds set at 20 dB-Hz, the results indicated zero availability for any individual constellation for both L1 and L5. Combined, there is coverage approximately 30 RE, approximately 50% of the cis-lunar distance (Figure 2). The visibility drop-off was due to the low C/N_0 and recommended a lower threshold at 15 dB-Hz.

Capuano[5] addressed this gap and described a simulated "Weak HEO" single frequency GPS L1 receiver with a 15 dB-Hz C/N_0 acquisition and tracking threshold for a representative MTO. The study used a GNSS Spirent for a Hardware-in-the-Loop setup and confirmed the feasibility of the receiver operating in cislunar space. The simulation assumed an antenna receiver of 10 dBi and stated that the carrier phase is affected by Doppler shifts and Doppler rates up to 60 KHz and 65 Hz/s at the beginning of the MTO, due to higher vehicle velocities, compared to the end of the MTO trajectory, with Doppler shifts and Doppler Rates no more than 20 KHz and 4 Hz/s respectively. The study also noted the code tracking thermal range jitter can be larger than 6 m due to the low C/N_0. The paper thoroughly describes the signal acquisition strategy and hardware. Signal acquisition will be challenging at the start of the MTO given the higher Doppler shifts and rates. The study did not provide further insights into the type nor dimensions of the GPS receiver antenna for the emulated 10 dBi receiver gain.

Delépaut[6] further investigated an interoperable weak signal GNSS single frequency receiver in a Deep Space Gateway (DSG) orbit, i.e., an Earth-Moon L2 Halo orbit. Using both Galileo and GPS detailed 3D antenna patterns, numerical simulations were performed for comparative analysis between the frequency bands E1/L1 and E5a/L5. Delépaut concluded that a high number of satellites were visible at Lunar altitudes using a receiver with a 14 dBi antenna and the same "Weak HEO" 15 dB-Hz C/N_0 acquisition and tracking threshold. The investigation provided the European Space Agency (ESA) plans for an In-Orbit Demonstration (IOD) of the use of the GNSS infrastructure at Lunar altitudes (from Earth), covering both CubeSat missions and the DSG.

This engineering note aims to extend and fill the gaps in the previous studies[3,4,5,6,7] for a small GNSS receiver transitioning Lunar vehicle specifically for a Cubesat form factor (12U to 16U) with an associated GNSS receiver antenna. The objective of this study is to investigate:

1. The minimum GNSS antenna form factor (antenna gain) that can be accommodated on a 12U Cubesat;

2. The position Dilution of Precision (PDOP) growth of a lunar bound space vehicle using a native medium-fidelity GNSS orbit dynamic and link simulator; and

3. The expected improvement of the PDOP during transition, assuming an interoperable GNSS receiver that can handle the GPS L1, L5, Galileo E1, E5a, E5b and the Beidou B1, B2a/B2.

The PDOP metric is a dimensionless figure of merit associated to the geometric resolution of the 3D position of the receiver to the visible GNSS signals, where a lower PDOP value is indicative of a higher position accuracy, excluding any receiver clock errors. Past GNSS cislunar studies have not quantified this metric for an MTO, which this paper will explore, inclusive of combined GNSS signals for an interoperable receiver. Timing errors and Geometric Dilution of Precision (GDOP) can be investigated in future studies.

L1, E1 and B1 has the common central frequency of 1575.42 MHz (high band). L5, E5a and B2a has a common central frequency of 1176.45 MHz (low band) and B2/2b and E5b (low band) has a common central frequency of 1207.14 MHz. The GLONASS system does not have exact common central frequencies although terrestrial interoperable receivers exist. The central frequencies for these three and other GNSS constellations are summarized in (Figure 4). Given the common central frequencies and that National Aeronautics Space Administration (NASA), European Space Agency (ESA) and China National Space Agency (CNSA) are vigorously planning a cadence of Lunar missions in the current and next decade, the remainder of this paper will focus only on these three GNSS. In particular, the selection of the three common central frequencies, resulting in a single physical interoperable GNSS antenna design. Other frequency combinations and constellations can be explored in future studies i.e., QZSS, IRNSS/NAVIC.

Section 2 describes the method, mathematical models and a new GNSS Lunar emulator to facilitate these investigations. Section 3 captures the parameters and results of the investigation while discussions of the results are documented in Section 4. Section 5 wraps-up this engineering note with the conclusion and future work.

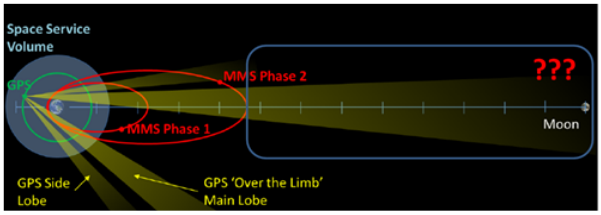

Figure 1: A visual representation (not to scale) of the potential sidelobes received at distances to the Moon. Visual modified from Parker[2]

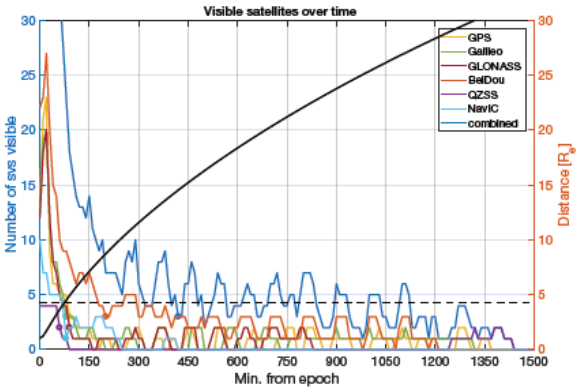

Figure 2: Signal visibility for a ballistic Lunar trajectory with 20 dB-Hz threshold at 30 RE (~50% of lunar distance)[4]

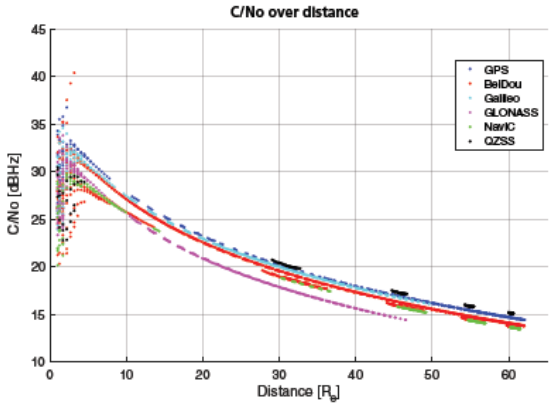

Figure 3: Simulated C/ N_0 for Lunar trajectory[4]

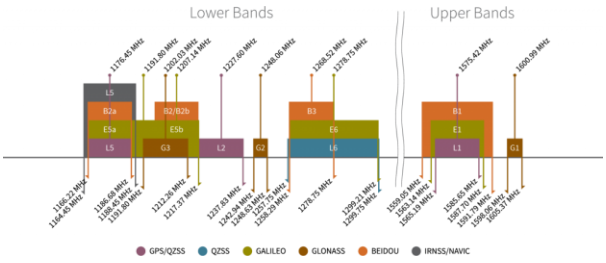

Figure 4: GNSS central frequencies[8]

METHOD, MATHEMATICAL MODELS AND NATIVE GNSS LUNAR SIMULATOR

The assessment approach taken by this engineering note is to perform a static link budget analysis, C/N_0, and Eb/N_0, for varying antenna diameters for the GPS L1, L5, and the common Galileo and Beidou signals. The

traditional parabolic and helix antennas have been selected for their notable high gains. Once the GNSS receiver antenna gain and form factor have been selected, the subsequent assessment is to determine the PDOP profile for the receiver transitioning from the Earth to the Moon i.e., the MTO, based on valid links of each GNSS SV constellations. All assessments are performed using the high-level language MATrix LABoratory (MATLAB).

Static Link Assessment

To determine the minimum GNSS receiver antenna size that can ensure a positive link at a maximum distance between the Lunar vehicle (LV) at maximum Lunar apogee and the GNSS space vehicle (SV), a sweep of the receiver antenna gain as a function of diameter was assessed based on several assumptions for the receiver characteristics as well as the link equation parameters. The criterion for a positive link is a C/N_0 acquisition and tracking greater than the design threshold for the carrier frequency. For a positive received energy-per-bit-to-noise-density ratio (Eb/N_0) probability of bit error rate (BER), a positive link is ensured when it is above a design threshold for the Bit Phase Shift Keying (BPSK) digital modulation at the given code rate.

The governing carrier phase link equation is given as:

$$\frac{C}{N0} = EIRP(\theta) - FSP - P_{pol} - P_{rxPoint} - P_{aRes} - P_{aFro} - P_{imp} + G_{aRx} - T_{total} - k \quad (1)$$

where

- *EIRP(θ)* is the effective isotropic radiated power of the GNSS SV transmitter offset by \theta from the transmitter boresight, which is nadir pointing.
- P_{Pol} is the polarization loss [dB];
- $P_{rzPoint}$ is the receiver pointing loss [dB];
- P_{aRes} is the receive antenna resistance loss [dB];
- P_{aFro} is the receive antenna front end loss [dB];
- P_{imp} is the receiver implementation loss [dB];
- G_{Rx} is the receive antenna gain [dBi];

The free space loss, where f_c is the transmitter central frequency is given as:

$$SP = 20\log_{10}(\frac{4\pi d f_c}{lightSpeed}) \quad (2)$$

The receive total temperature noise [dBK][9] is given as:

$$T_{total} = 10\log_{10}(\alpha T_{ant} + (1-\alpha)T_0 + T_{sys}) \quad (3)$$

where:

- α is the fractional attenuation of cable
- T_{ant} is the antenna temperature [K]
- $T_0 = 290$ K
- $T_{sys} = T_0(10^{\frac{NF}{10}} - 1)$
- *NF* is the Noise Figure
- k is the Boltzmann constant in decibels [dBW/K-Hz]

Note that Delépaut[6] assumes an approximate noise figure of 2.95, resulting is a T_{sys} of 282 K. With an assumed T_{ant} of 113 K, the total temperature noise would be 395 K, which would be high for an antenna in the MTO if not Sunward facing. Delépaut also ignored implementation and cable losses. Winternitz[3] on the other hand used the MMS in-orbit values, with T_{sys} of 132 K and T_{ant} of 34 K, resulting in a total temperature noise of 166 K. The link assessment shall use the MMS, given the more representative antenna and system noise values.

The receiver antenna gain is a function of the type of antenna. The empirical models[10] for both the parabolic and helix antennas peak gain and half-power beamwidth are given in (Table 1).

Table 1: Receiver antenna model equations

Parameter	Parabolic	Helix*
Peak gain[1] [dBi]	$17.8 + \log_{10}(\mathrm{D}) + 20\log_{10}(f)$ $\eta = 0.55$	$10.3 + 10\log_{10}(C^2L/\lambda^3)$, $C = \pi D$ $\eta = 0.70,\ 0.8 \le C/\lambda \le 1.2$ $52/\sqrt{C^2L/\lambda^3}$
Half-power beamwidth [deg]	$21/fD$	$52/\sqrt{C^2L/\lambda^3}$

*D is the diameter [m], L is the Length [m], λ is the central wavelength [m] and f is the central frequency [GHz].

Note that the receiver pointing loss is a function of the antenna pointing error θ and the half-power beamwidth HPBW:

$$P_{rzPoint} = -0.12(\frac{\theta}{HPBW(f)}), \text{[dB]} \quad (4)$$

The free space loss is a function of the expected maximum distance between the lowest altitude GNSS

constellation and the LV GNSS receiver at Lunar apogee. This distance is determined through trigonometry as shown in (Figure 5), where the angular radius of the Earth for both the SV and the LV Line of Sight (LoS) grazing the Earth limb radius (above the atmospheric density) is determined. The sum of the cosine between the SV and LV to the midpoint of the Earth Limb tangent is the distance between the SV and the LV.

$$\rho_{SV} = (R_E + Atm)/R_{SV} \tag{5}$$

$$\rho_{LV} = (R_E + Atm)/R_{LV} \tag{6}$$

$$R_{SV/LV} = R_{SV}\cos(\rho_{SV}) + R_{LV}\cos(\rho_{LV}) \tag{7}$$

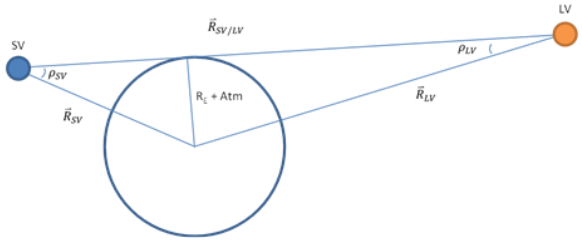

Figure 5: Geometry of LV and SV

The code link equation is given as

$$\frac{Eb}{N_0} = \frac{C}{N_0} - 10\log_{10} R, \tag{8}$$

Where R is the code data rate.

GNSS Position Emulator in cislunaR Space (GPERS)

The GNSS Position Emulator in cislunaR Space (GPERS) is a native MATLAB script that executes a Simplified General Perturbation 4 and 8 (SGP4 / SGP8) orbit propagation of the GNSS two-line-element (TLE) constellations as well as other TLE's such as the MMS spacecraft and the conceptual Lunar space vehicle. The emulator also propagates the Moon's position. The International Terrestrial Reference Frame (ITRF) at Julian date (JD)2000 and JD monotonic time is used for the epoch and simulated timesteps. The simulator propagates the LoS between the GNSS SVs and the LV vectors to determine any Earth occultation as well as the SV transmitter dynamic off-boresight EIRP (Figure 6) and the GNSS receiver on the LV off-boresight gain. For simplicity, a mean EIRP from the GPS L1 Block IIF as shown in (Figure 7) was assumed for all SV's regardless of constellation type, i.e., all GPS, Galileo or Beidou uses the same EIRP pattern. The simulator calculates the link access for each SV as well as the PDOP for the valid SV links that are above the C/N_0 threshold, and the assessment of the Eb/N_0. The simulator currently does not simulate pseudocode generation nor an acquisition model. The simulator also does not account for any Lunar occultation. The GPERS code snippet is captured in (Figure 8). The SGP4 / SGP8 model is described further in the Celestrek site[11].

The dilution of precision is (DOP) is essentially a metric used to describe the precision of the GNSS transmitter to GNSS receiver geometry for point positioning. The DOP is derived from the diagonal (trace) of the covariance matrix M, of adjusted parameters derived from the linearized observation mode; The position DOP (PDOP) consists only of the first three position elements σ_x. σ_y, σ_z. The covariance matrix is generated from the epoch-by-epoch linear least square matrix A[12] of the linearized pseudo-range P at that epoch in ITRF:

$$A = \begin{bmatrix} \frac{\partial P_1}{\partial x} & \frac{\partial P_1}{\partial y} & \frac{\partial P_1}{\partial z} & c \\ \frac{\partial P_2}{\partial x} & \frac{\partial P_2}{\partial y} & \frac{\partial P_2}{\partial z} & c \\ \vdots & \vdots & \vdots & \vdots \\ \frac{\partial P_n}{\partial x} & \frac{\partial P_n}{\partial y} & \frac{\partial P_n}{\partial z} & c \end{bmatrix} \tag{9}$$

$$M = (A^T A)^{-1} = \begin{bmatrix} \sigma_x^2 & \sigma_{xy}^2 & \sigma_{xz}^2 & \sigma_{xt}^2 \\ & \sigma_y^2 & \sigma_{yz}^2 & \sigma_{yt}^2 \\ & \therefore & \sigma_z^2 & \sigma_{zt}^2 \\ & & & \sigma_t^2 \end{bmatrix} \tag{10}$$

$$PDOP = \sqrt{\sigma_x^2 + \sigma_y^2 + \sigma_z^2} \tag{11}$$

Where c is the speed of light.

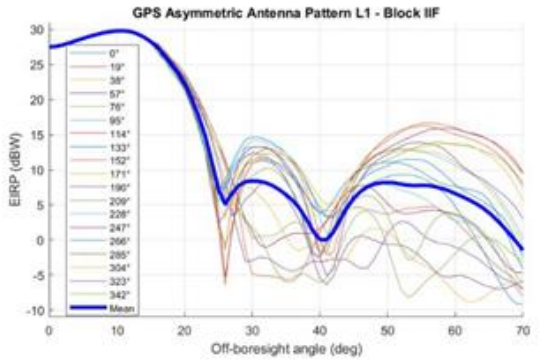

Figure 6: GPS L1 Block IIF [9] EIRPS as a function of off-boresight angle: published EIRP patterns

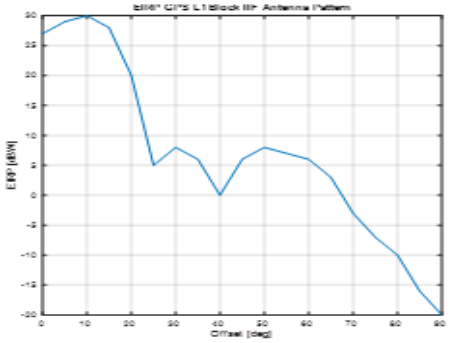

Figure 7: GPS L1 Block IIF [9] EIRPS as a function of off-boresight angle: approximated mean EIRP

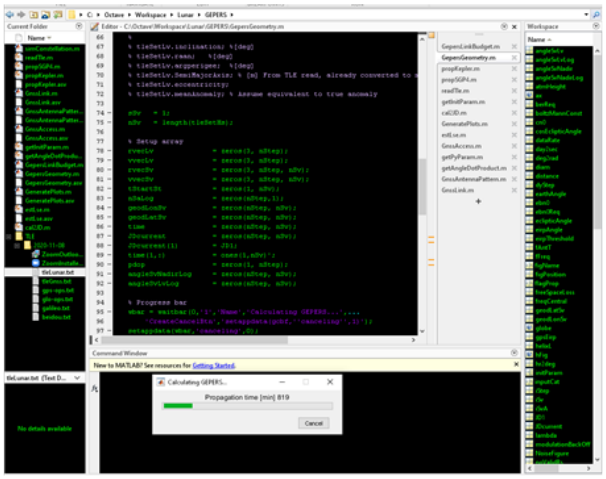

Figure 8: GNSS Enabled Position Estimation in cislunaR Space (GEPERs) Simulator

ASSESSMENT PARAMETERS AND RESULTS

The parameter values for the static link assessment, shown in (Table 4) of the Appendix, re-uses several values based on the analysis performed by Delépaut[7]. Variations include the use of the BDS frequencies and the receiver temperature noise model. The target C/N_0 threshold was set to 15 dBHz, as used by Capuano[5] and Delépaut[7] . The allowable bit error probability was selected for 10^{-5}, which corresponds to an Eb/N_0 requirement of 5 dB for the BPSK modulation applied to the GPS, Galileo and Beidou data rates of 50 bps, 448 bps and 100 bps respectively. An off-nadir boresight of 24° corresponds to approximately the half-power beamwidth, i.e., the edge of the GNS SV EIRP primary lobe. This translates to the pointing loss from the peak EIRP and emulates the worst-case side lobes seen by the LV GNSS receiver. Note that the analysis assumes a receiver pointing error of 4.156° from Nadir at the maximum distance. For the helix antenna, the length was fixed at 200 mm, equivalent to 2U, which is a practical length for a 16U Cubesat.

The antenna diameter sweeps for both the parabolic and helix antennas for different central frequencies of GPS L1, L5 at 50 bps, Galileo E5a at 448 bps, and Beidou B2a at 100 bps were performed to determine positive Eb/N_0 margins at a static 60 RE Lunar distance. As expected, a smaller diameter helix antenna, at fixed lengths of 200 mm, closes the bit-error rate link relative to a parabolic antenna. (Figure 9) to (Figure 13) shows the identification process for the minimum diameter of the Helix antenna at 0 dB Eb/N_0, summarized in (Table 3). It is clear that a lower data rate requires a small diameter receiver antenna and that the smallest diameter interoperable antenna is 130 mm, but only for the common central frequency (upper band) 1575.42 MHz i.e., L1, E1, B1. A larger antenna up to 760 mm diameter would be needed to cover 1207.14 MHz (lower band) i.e., E5b and comfortably for B2/2b. Heritage deployable helix antennas that can be stowed within 1U are now commercially available e.g., Oxford space systems[13] and is an ideal candidate to realize such an antenna for a Cubesat destined for the Moon. Recall that the sweeps assessment used a fixed length of 200 mm, hence a balanced diameter to length ratio should be investigated in the future for a more efficient 3 dB antenna gain pattern.

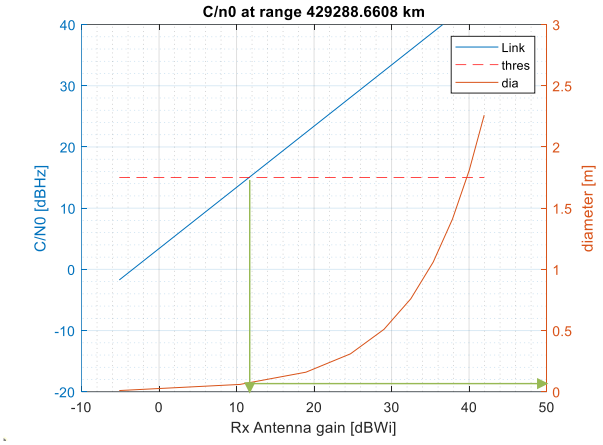

Figure 9: GNSS Receiver GPS L1 Eb//N_0 vs antenna diameter: (d) Helix with 0.2 m length

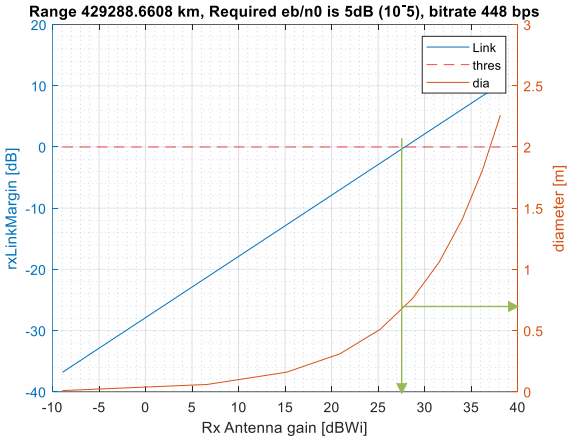

Figure 12. GNSS Receiver Galileo E5a Eb/N0 vs antenna diameter: helix with 0.2m length

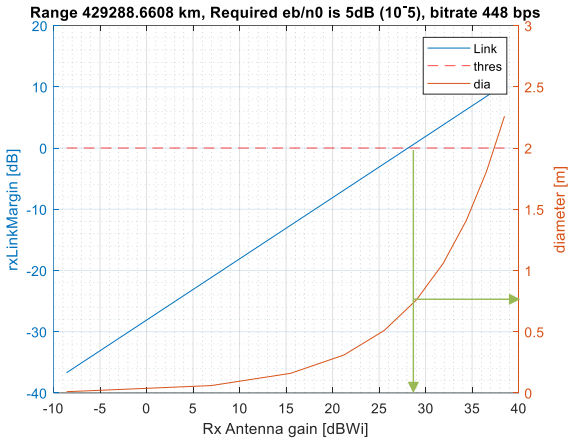

Figure 10: GNSS Receiver Galileo E5b Eb/N_0 vs antenna diameter: (d) Helix with 0.2 m length

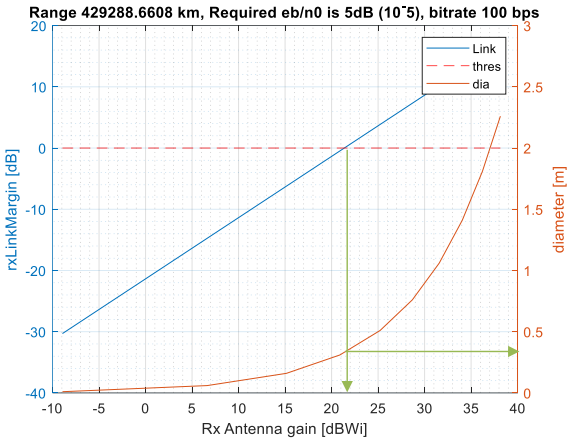

Figure 13. GNSS Receiver Beidou B2/2b Eb/N_0 vs antenna diameter: helix with 0.2 m length

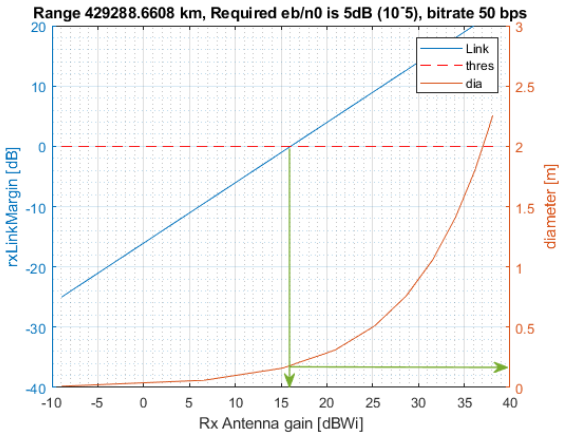

Figure 11. GNSS Receiver GPS L5 Eb/N_0 vs antenna diameter: helix with 0.2 m length

Table 2: Receiver antenna model equations

Case	Rate [bps]	Parabolic [m]	Helix** [m]
GPS L1 Eb/N_0	50	0.70	0.13
Galileo E5b Eb/N0	448	1.87	0.76
GPS L5 Eb//N_0	50	0.71	0.18
G/B E5a Eb/N_0	448	N/A	0.70
G/B B2/2b Eb/N_0	100	1.27	0.35

**Helix length = 0.2 m

The GPERS simulator generates an orbit visualization of the GNSS constellations, the position of the Moon at

the end of the simulation time and the MTO trajectory, simplified to an ellipse versus the more common 'figure 8' as shown in (Figure 14). The LV carrying the GNSS receiver starts from a near parking orbit and transitions slightly beyond the Moon. The GPERS simulation parameters are shown in Table 3 in the Appendix. The subsequent (Figure 15) captures the number of valid individual GNSS constellation SV's accessed by the GNSS receiver for both carrier and code for a single Helix antenna with a diameter of 130 mm and a length of 200 mm pointed towards Earth (Nadir tracking). (Figure 16) to (Figure 27) captures the theoretical interoperable performance to close the Eb/N_0 link margins for various combinations of valid GNSS SV constellations; the more stringent requirement than the C/N_0 link margin performance. Discussions of the dynamic link performance are captured in the next section.

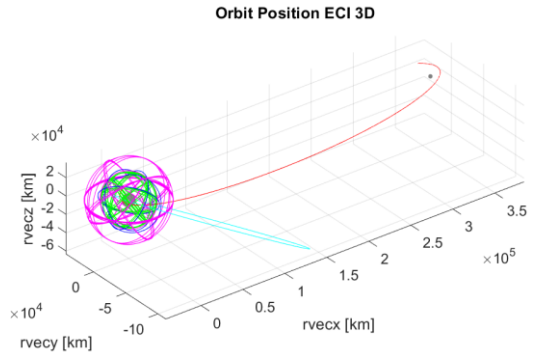

Figure 14: GPERS visualization to scale: GNSS constellations and Moon Transfer Orbit (MTO) with MMS#4

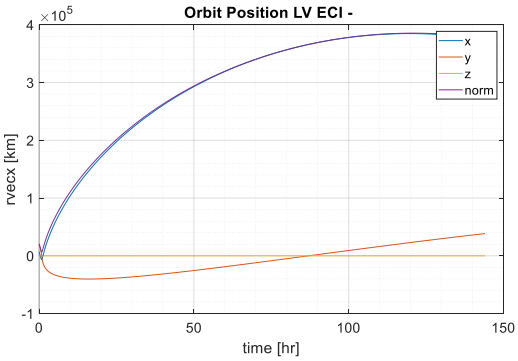

Figure 15: GPERS visualization to scale: (b) MTO time series

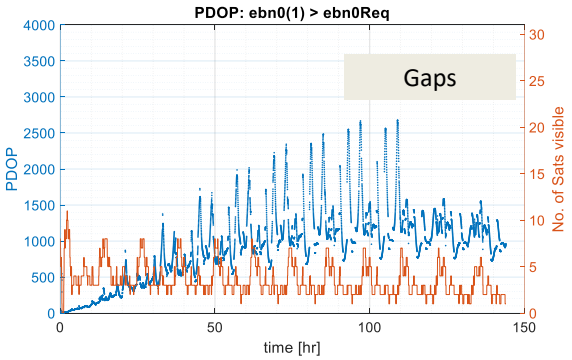

Figure 16: Individual GNSS constellation DOP GPS L1 EB/N_0

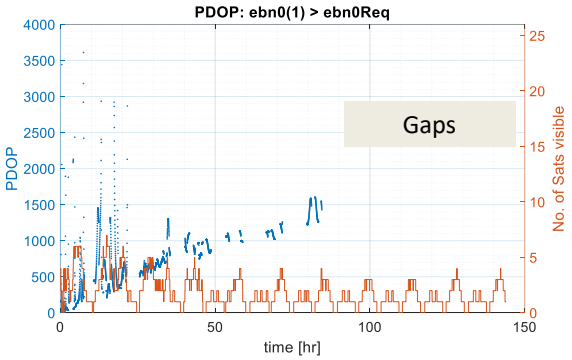

Figure 17: Individual GNSS constellation DOP Galileo E5b Eb/N_0

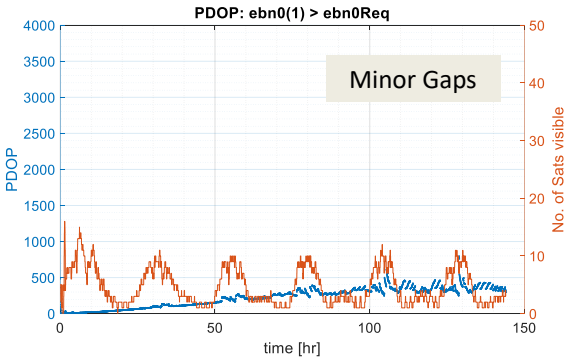

Figure 18: Individual GNSS constellation DOP Beidou Eb/N_0

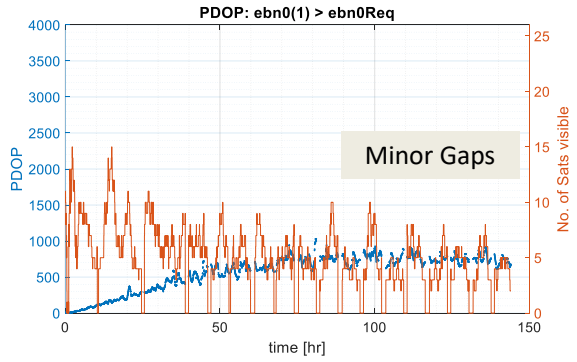

Figure 19: Interoperable GNSS Receiver DOP GPS L1 + Galileo E5b Eb/N0

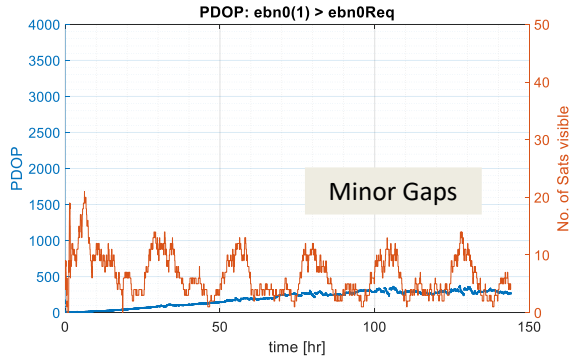

Figure 20: Interoperable GNSS Receiver DOP Galileo E5b + Beidou 2/2b E5b Eb/N0

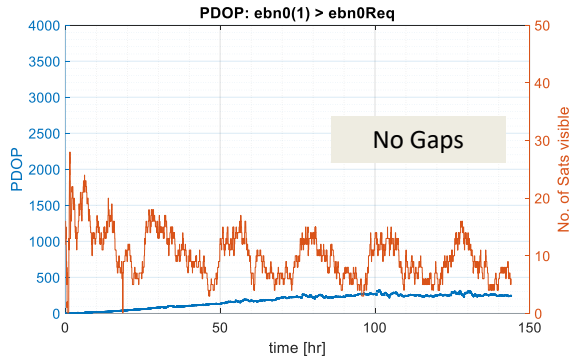

Figure 21: Interoperable GNSS Receiver DOP GPS L1 + Galileo E5b + Beidou 2/2b Eb/N0

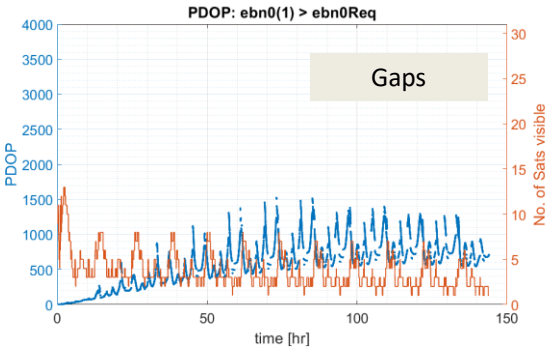

Figure 22: Individual GNSS constellation DOP GPS L5 Eb/N0

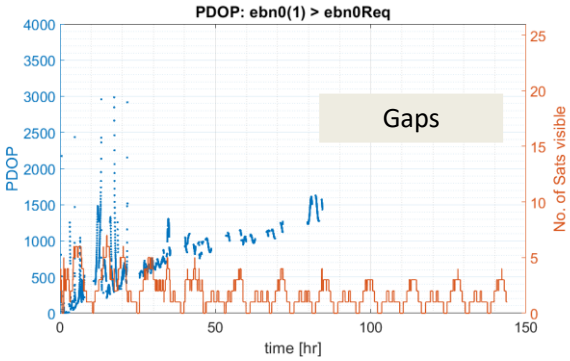

Figure 23: Individual GNSS constellation DOP Galileo E5a Eb/N0

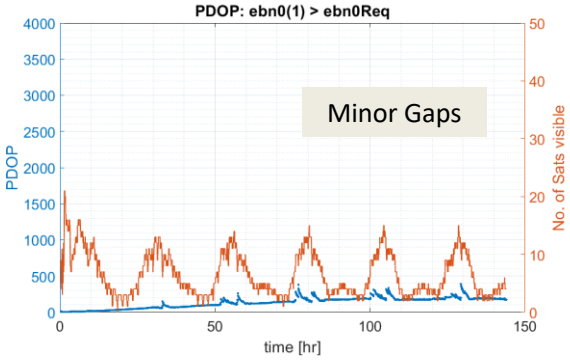

Figure 24:Individual GNSS constellation DOP Beidou B2a Eb/N0

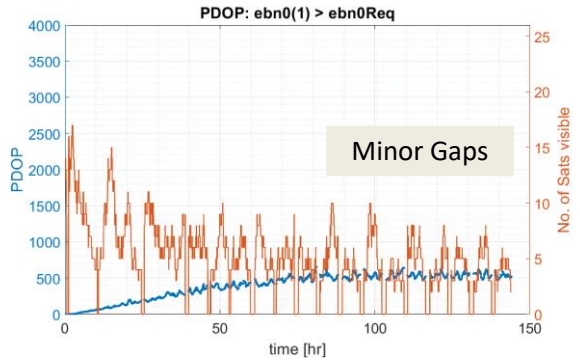

Figure 25: Interoperable GNSS Receiver DOP GPS L5 + Galileo E5a EB/N_0

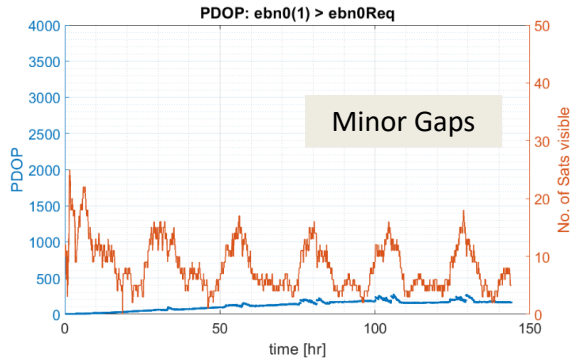

Figure 26 Interoperable GNSS Receiver DOP Galileo E5a + Beidou B2a Eb/N_0

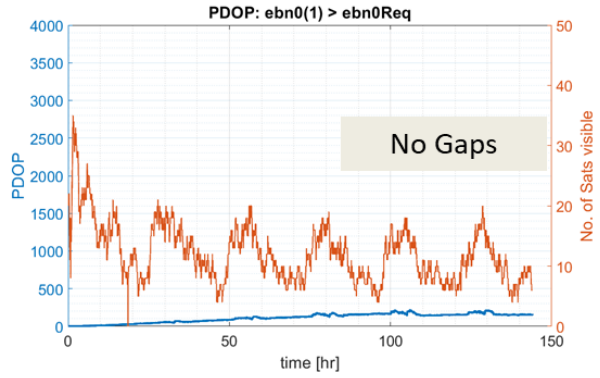

Figure 27 Interoperable GNSS Receiver DOP GPS + Galileo + Beidou (L1 + E5b + B2/2b) Eb/N_0

DYNAMIC LINK DISCUSSION

From (Figure 16) to (Figure 18) and (Figure 22) to (Figure 24), the individual GNSS PDOP grows as the number of valid GNSS SV reduces with the increasing trajectory of the LV. The orbital nature of the constellation resulted in a sinusoidal number of valid SV links for both the C/N_0 and EB/N_0. This phenomenon, however, has a minor impact to the PDOP trend. Traditional terrestrial PDOP values of less than 20 are measures of higher accurate position estimates. In the case of the LV MTO, the PDOP can reach 500 for the carrier and 1000 for the code. Sudden drops of valid SV link to less than 3 results in PDOP 'spikes' above 500. The carrier PDOP for the Galileo constellation, however, are consistently below 500 with an exception nearing the MTO apogee, where valid SV's of one or less caused invalid PDOP calculations. The code PDOP is worse and is not unexpected as Galileo's data rate is 8 times that of the GPS data rate. The Beidou constellation was simulated with the same parameters as Galileo, albeit with a data rate of 100 bps, and performs much better with carrier PDOP in the 120 range and code PDOP below 300 at the MTO apogee. This is predominantly attributed to the unobstructed GNSS receiver LoS to the Beidou SV given the existence of the Beidou SV's in four geosynchronous orbit planes, resulting in larger SV to LV GNSS receiver angular separation.

For an interoperable GNSS receiver, (Figure 19) to (Figure 21) as well as (Figure 25) to (Figure 27) shows PDOP performance improvements for all combinations, i.e. GPS + Galileo, Galileo + Beidou, GPS + Galileo + Beidou for L1, E5b, B2/2a and L5, E5a, E5b. The increased number of SV reduces carrier PDOPs to below 200 and code PDOP to below 400. Gaps still exist for the GPS + Galileo and Galileo + Beidou for the code PDOP. The inclusion of all three constellations is shown to ensure code PDOP below 120 without gap throughout the MTO. More importantly, the ability to close the link loop at the lower bands, E5b + B2b, and L5 + E5a + B5a with the small GNSS helix antenna allows the ability to resolve signal ambiguities.

Even with an interoperable receiver using all three GNSS constellations, the PDOP values at the end of the MTO will still equate to position estimation confidence to several thousands of kilometers which necessitates an additional orbit estimation strategy to refine the accuracy, such as a full state extended Kalman filter, to ensure continuous and improved orbit (and clock predictions), similar to NASA Goddard's GEON estimator operating on MMS.

CONCLUSION

This investigation provides additional information, filling the gaps found in previous studies for a GNSS receiver transitioning from the Earth to the Moon. This investigation also confirms that an interoperable receiver, particularly the inclusion of the Beidou constellation with its four geosynchronous constellation planes coupled to the GPS and Galileo constellations improves PDOP significantly. Utilization of all three constellation provides a continuous and low carrier and

code PDOP at less than 200 even at MTO apogee. An onboard estimator like NASA Godard's GEONs is still required, and with the improved PDOP, this interoperable GNSS receiver is expected to provide even better performances than predicted by Winternitz[3].

This investigation also confirms the feasibility of a small nadir pointing 130 mm diameter by 200 mm length helix GNSS antenna for a 16 U Cubesat. A concept to modify a flight-heritage deployable helical antenna from Oxford Space System [12] to the minimum dimensions assembled on a flight-heritage Nanoavionics 16U platform [13] as a representative example for a Lunar Vehicle Cubesat is shown in (Figure 28). With the identified elements, and this preliminary investigation, the main author is confident that a GNSS Lunar receiver Cubesat mission can be potentially realized within the next 2 years for a high-risk mission tolerance. More notably, the non-reliance of such a Cubesat mission and the cadence of more Lunar bound spacecraft and Lunar orbiters that choose to incorporate a GNSS interoperable receiver and antenna system will minimize the reliance on NASA's Deep Space Network (DSN) for two-way ranging and any onboard stellar compass for navigation.

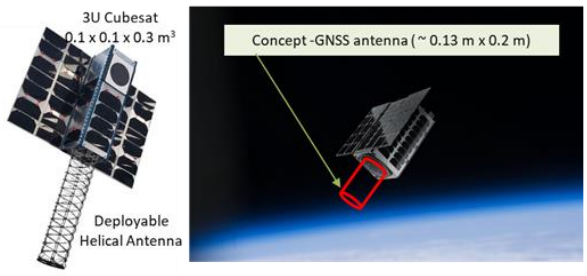

Figure 28: Representative xample concept of a GNSS enabled receiver for the Cis-lunar Space. 16U CubeSat based on a Nanoavionics platform[14] using an Oxford Space Systems' flight heritage deployable Helix Antenna[13]

The following list the future work that can be pursued from this engineering note:

- Use more representative GNNS SV transmit EIRPs, particularly for the Galileo and Beidou constellations;
- Inclusion of the GLONASS constellation TLEs as well as other constellations;
- Model receiver clock errors (bias and drift), weak signal and code acquisition models for GPERs and re-assess the performance with single and interoperable constellations;
- Develop the ubiquitous extended Kalman filter and explore an unscented Kalman filter to estimate position, velocity and clock errors; and
- Investigate Deep Learning algorithms to potentially improve cislunar trajectory correction maneuvers for various operational scenarios

Acknowledgments

The main author would like to thank God, his wife and children for their patience and support.

References

1. NASA Artemis Program https://www.nasa.gov/what-is-artemis (accessed on 06-Oct-2020).
2. Parker J., et al, "An introduction to High-Altitude Space Use of GNSS (For Timing People)", NASA, 58th Civil GPS Service Interface Committee Timing Subcommittee, Miami, USA, September 24, 2018.
3. Winternitz L., et al, "GPS Based Autonomous Navigation Study for the Lunar Gateway", AAS 19-096, Annual American Astronautical Society, Guidance, Navigation and Control Conference, Breckenridge, Colorado ,USA, Jan 13, 2019.
4. United Nations Office for Outer Space Affairs (OOSA), "The interoperable Global Navigation Satellite Systems Space Service Volume, 2018
5. Capuano, "Standalone GPS L1 CA Receiver for Lunar Missions", Sensors (Basel), 2016 Mar 9, pp. 347, sensors-16-0034.
6. Delépaut et. Al, "Use of GNSS for lunar missions and plans for Lunar In-Orbit Development", Advances in Space Research,Vol. 66m Issue 12, 15 Dec 2020, P 2739-2756.
7. Delépaut et. Al, "A System Study for Cislunar Radio Navigation Leveraging the Use of Realistic Galileo and GPS Signals", 32nd International Technical Meeting of the Satellite Division of the Institute of Navigation (ION GNSS+ 2019) Miami, Florida, September 16-20, 2019.
8. Tallysman, "GNSS Constellations, Radio Frequencies and Signals" https://www.tallysman.com/gnss-constellations-radio-frequencies-and-signals/ (accessed on 26-May-2022).
9. Langley, "Gps Receiver System Noise", GPS World, June 1997.

10. Wertz, “Space Mission Analysis and Design”, 3rd edition, 1999, Microcosm.

11. Celestrek, https://celestrak.com/, (accessed on 08-Nov-2020).

12. Bisnath S., “Topic 8, GNSS Point Positioning”, ESSE 3670: “Global Navigation Satellite Systems, Winter 2019, Dept. of Earth & Space Science & Engineering, Lassonde School of Engineering, York University

13. Oxford Space Systems Deployable Helix Antenna, https://oxford.space/helical/, (accessed on 29-Nov-2020).

14. Nanoavionics, https://nanoavionics.com (accessed on 19-Nov-2020)

15. BeiDou Navigation Satellite System Signal In Space Interface Control Document, Open Service Signal B1I (Version 3.0), China Satellite Navigation Office, February 2019

Parameter	GPS L1	Galileo / Beidou E5b	GPS L5	Galileo / Beidou E5a	Unit
NoiseFigure	2.95	2.95	2.95	2.95	dB
temp0	290	290	290	290	K
rxSysNoiseTemp	132	282	132	282	K
rxAntNoiseTemp	34	113	34	114	K
rxImplmentLoss	-1.7	-1.7	-1.7	-1.7	dB
rxAntResisLoss	-0.25	-0.25	-0.25	-0.25	dB
rxAntFrontLoss	-1	-1	-1	-1	dB
rxHpbw	12.2	12.2	12.2	12.2	deg
rxPointErr	4.156	4.156	4.156	4.156	deg
dataRate	50	448 (Galileo) 100 (Beidou)	50	448 (Galileo) 100 (Beidou)	bps
berReq	1.00E-05	1.00E-05	1.00E-05		
ebn0Req	5	5	5		dB

Appendix

Table 3: GEPERS simulation parameters

Parameter	Value
TLE epoch	2020-11-08
Sim start	2024-06-22 12:00:00
Sim end	2024-06-28 12:00:00
tleSetLv.inclination	0.0°
tleSetLv.raan	168.2627°
tleSetLv.eccentricity	0.9664
tleSetLv.argperigee	0.0°
tleSetLv.meanAnomoly	212°
tleSetLv.meanMotion	0.10 rev/day
tleSetLv. SemiMajorAxis	196,039km
Link parameters	Table 4
GNSS antenna type	Helix 0.13 m dia, x 0.2 length m
GNSS antenna attitude	Nadir pointing throughout MTO

Table 4: GPS , Galileo and Beidou link parameters

Parameter	GPS L1	Galileo / Beidou E5b	GPS L5	Galileo / Beidou E5a	Unit
Frequency	1575.42	1207.14	1176.45	1176.45	MHz
txEirpPeak	22	19.7	22	19.7	dBW
txHpbw (half power)	24	24	24	24	deg
txLineLoss	-1	-1	-1	-1	dB
sideLobe	25	25	25	25	Deg
rxFracAtt	1	1	1	1	